Am J Cancer Res 2022;12(4):1502-1510
www.ajcr.us /ISSN:2156-6976/ajcr0139304

Original Article

The efficacy and mechanism of thoracic photodynamic therapy mediated by hematoporphyrin injection on disseminated pleural malignancies of Lewis lung carcinoma in mice

Wenjuan Pu[1,2*], Lei Xue[1*], Ziqi Han[1], Lei Yang[1], Yubao Wang[3], Nansheng Wan[1], Jing Feng[1]

[1]Department of Respiratory and Critical Care Medicine, General Hospital of Tianjin Medical University, Tianjin 300052, China; [2]Department of Respiratory and Critical Care Medicine, Tangdu Hospital, Air Force Military Medical University, Xi'an 710038, Shaanxi, China; [3]Institute of Infectious Diseases, The Second Hospital of Tianjin Medical University, Tianjin 300211, China. [*]Equal contributors.

Received September 22, 2021; Accepted January 26, 2022; Epub April 15, 2022; Published April 30, 2022

Abstract: In order to avoid the problems of long exposure time and high incidence of photosensitivity by intravenous injection of photosensitizer, our study explore the safety, efficacy, and possible mechanisms of photodynamic therapy (PDT) by intrathoracic administration of hematoporphyrin injection in the treatment of disseminated pleural malignancies of Lewis lung carcinoma in mice to provide a theoretical basis for thoracic PDT in the clinic. Hematoporphyrin was administered into the thoracic cavity of tumor-bearing mice, and the concentrations of hematoporphyrin in normal and tumor pleural tissues were detected by high-performance liquid chromatography. The tumor-bearing mice were randomly divided into four groups: model control, pure laser irradiation, PDT low-dose, and PDT high-dose groups. Hematoxylin and eosin (H&E) staining was used to observe the histological changes in normal pleural tissue. H&E and DNA in situ nick end-labeling staining were used to detect necrosis and apoptosis in the tumor tissues. The tumor volume in each group from high to low was as follows: model control group > pure laser irradiation group > PDT low-dose group > PDT high-dose group. Inflammatory cells infiltrated the normal pleural tissue of the PDT group. Necrosis was observed to different extents in the tumor tissues of the PDT group. The apoptosis index of each group from high to low was as follows: PDT high-dose group > PDT low-dose group > pure laser irradiation group > model control group. The differences were statistically significant ($P<0.05$). Hematoporphyrin selectively accumulated in tumor pleural tissues. PDT with intrathoracic administration of hematoporphyrin injection could inhibit the thoracic implant tumors in mice by inducing necrosis and apoptosis.

Keywords: Photodynamic therapy, photosensitizer, thoracic implant tumor, necrosis, apoptosis

Introduction

According to statistics, pleural spread of non-small cell lung carcinoma (NSCLC) occurs in 10-50% of patients during the course of lung cancer, and the median survival of patients with pleural spread of NSCLC is usually 6-9 months [1]. Currently, the treatment methods for lung cancer include surgery, chemotherapy, radiotherapy, molecular targeted therapy, and immunotherapy, along with several other options [2]. Surgical treatment is the first choice for patients with early-stage lung cancer [3]. However, more than 20% of patients with early lung cancer cannot undergo surgery because of advanced age, severely impaired lung function, and other complications [4]. It is usually difficult to operate in patients with advanced lung cancer due to uncontrolled invasion and metastasis.

As a minimally invasive treatment method, photodynamic therapy (PDT) has been increasingly used against malignant tumors. The basic principle of PDT is that when the photosensitizer selectively accumulates in the diseased tissue, the tissue is irradiated with a light source of a specific wavelength, and the photochemical

reaction occurs, destroying tumor cells [5, 6]. PDT has been used to treat various cancers, including lung, head and neck, brain, pancreas, abdominal cavity, breast, prostate, skin, and liver cancers [7-9]. Based on previous studies, PDT is feasible and effective in the treatment of diffuse malignant tumors in the thoracic or peritoneal cavity, bladder, and brain [10-15].

In the 1970s, hematoporphyrin derivatives as photosensitizers were successfully applied to the treatment of bladder cancer, which created a precedent for PDT to treat tumors [16]. The photosensitizers discovered so far that can be used for photodynamic therapy can be roughly divided into three generations according to the chronological order of appearance. The photosensitizers used for lung cancer treatment mainly include hematoporphyrin, Photofrin, and NPe6. However, only the first generation of hematoporphyrin is available in domestic markets; therefore, we chose hematoporphyrin as the photosensitizer in this experiment. When these drugs available, we will also choose other photosensitizers in the future.

Common complications of PDT mediated by hemoporphyrin injection in the treatment of respiratory tumors include photosensitive reaction, cough, dyspnea, fever, and hemoptysis, among which the incidence of photosensitive reaction is the highest, ranging from 5% to 28% [17-19]. Therefore, patients need to be protected from light for a long time after PDT, which brings a lot of inconvenience to daily life [20, 21]. Studies have shown that photosensitizers can enter the body through intravenous, intraperitoneal, and percutaneous local injections and are eventually absorbed by tumor cells [22]. Our study aimed to explore the application of thoracic photodynamics in pleurally disseminated disease and malignant pleural effusion. To avoid the problems of long exposure time and high incidence of photosensitivity by intravenous injection of photosensitizers, we used intrathoracic administration of hematoporphyrin injection and explored the efficacy and possible mechanisms of this PDT approach in the treatment of diffuse NSCLC.

Materials and methods

The animal experimental procedure was approved by the Model Animal Research Center of Tianjin Medical University General Hospital and was conducted in accordance with the Institutional Animal Care and User guidelines.

Animals

C57BL/6 male mice (6-8 weeks old, weight of 20-22 g) were purchased from SPF Biotechnology Company (Beijing, China). The animals were kept at a constant temperature (22-25°C) and humidity (30-45%) in the room.

Reagents and instruments

Hematoporphyrin (Xiporfin) was purchased from Chongqing Milelonge Biopharmaceutical Company (China). The DNA in situ nick end-labeling (TUNEL) kit was purchased from Roche (Basel, Switzerland). The photodynamic therapy instrument was manufactured by the Guilin Xingda Optoelectronic Medical Equipment Company (China). The output wavelength was 630 nm. The mode of operation was continuous and adjustable from 0 to 780 mW.

Cell culture

The Lewis lung carcinoma cell line (LLC) was purchased from the Cell Bank of the Chinese Academy of Sciences (Shanghai, China). The recovered mouse Lewis lung cancer cells were cultured in a high-glucose DMEM medium with 10% (v/v) fetal calf serum, 100 U/mL penicillin, and 100 μg/mL streptomycin. The cells were then cultured in an incubator at 37°C and 5% CO_2. The cell concentration was adjusted to 2.5×10^5 cells/50 μl cell suspension using PBS.

Thoracic implant tumor models

Based on our previous research, the mice were injected with 5×10^5 cells/100 μL cell suspension percutaneously into the right lateral thorax at the dorsal axillary line approximately one centimeter above the caudal edge of the ribcage, with a depth of approximately 5 mm. During our repeated exploration and operation, the absence of bubbles through the negative pressure back syringe indicated successful injection of the cell suspension into the thoracic cavity. The respiration of the mice was monitored during injection. Eight days after the inoculation of LLC cells, the animals were visualized using the Inliview-3000B animal positron emission tomography-computed tomography (PET-CT) device to observe the tumors in the thoracic cavity.

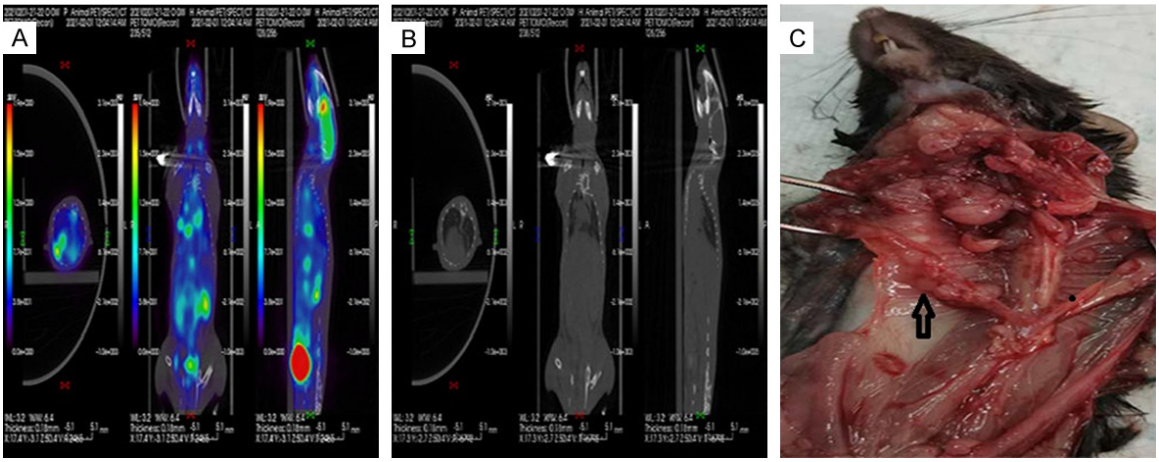

Figure 1. PET image of tumor model in mice showed that there were multiple radioactive concentrated shadows in the thoracic cavity of mice (A). CT image of tumor model in mice showed that there were multiple space-occupying lesions in the thoracic cavity of mice, and the boundary with hilum of lung was not clear (B). Representative tumor burden 8 days after inoculation with LLC cells. Black arrows indicate millimeter-sized nodules exposed on the surface of the pleura after lung and heart resection (C).

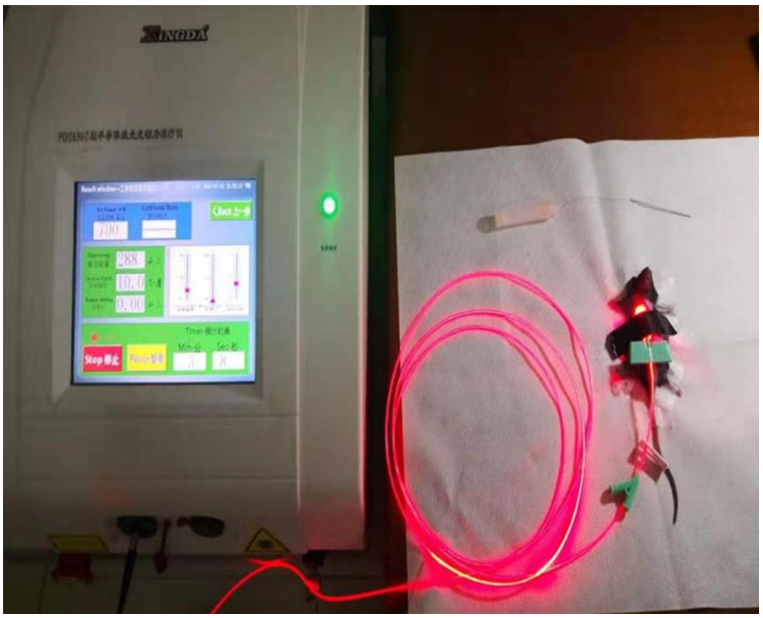

Figure 2. The process of PDT.

Determination of hematoporphyrin concentration injected into the thoracic cavity

Hematoporphyrin at a dose of 10 mg/kg was slowly injected into the thoracic cavity. The mice were dissected after 4 h of injection, and hematoporphyrin concentrations in normal and tumor pleural tissues were determined by high-performance liquid chromatography (HPLC).

Photodynamic therapy

The model was considered to be successfully established when the PET-CT images showed multiple radioactive concentrating shadows in the thoracic cavity (**Figure 1**). After 9 days of cell inoculation, 24 tumor-burdened mice were randomly divided into four groups: the control group (no photosensitizer, no laser irradiation), the pure laser irradiation group (with laser irradiation but without photosensitizer), the PDT low-dose group (laser irradiation after photosensitizer at a dose of 5 mg/kg), and the PDT high-dose group (laser irradiation after photosensitizer at a dose of 10 mg/kg was administered). The same as tumor modeling, hematoporphyrin was injected into the right thoracic cavity of mice. After protection from light for 4 h, illumination of the thoracic cavity was accomplished using a cylindrical diffusing fiber (active length: 1 cm; diameter: 200 μm) (**Figure 2**). Illumination was performed using a 630 nm diode laser for 10 min at a power of 700 mW.

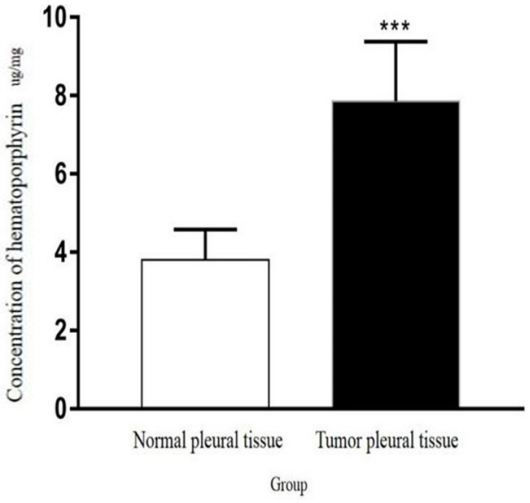

Figure 3. Determination of hematoporphyrin concentration in normal pleural tissue and tumor pleural tissue. The mean concentrations of hematoporphyrin in normal pleural tissue and tumor pleural tissue were 3.965 ug/mg and 7.854 ug/mg by HPLC 4 h after injection of hematoporphyrin injection into the thoracic cavity. The concentration of hematoporphyrin in tumor pleura tissue was significantly higher than that in normal pleura tissue, and the difference was statistically significant (***P<0.001).

Evaluation of the effect of PDT

After 48 h of PDT, PET-CT was performed again to evaluate the efficacy. The comparison of PET-CT images and assessment of tumor spatial distribution were performed by professional radiologists. Thereafter, the mice were sacrificed by cervical dislocation. The thoracic cavity of mice was opened to further observe the spatial distribution of tumors. Digital photographs were used to record the spatial distribution of tumors. Tumors on the pleural surface, pulmonary hilar and mediastinal lymph nodes, and other tumor nodules visible to the naked eye were completely extracted. The length and short diameter of the tumors were measured with a vernier caliper, and the volume of single tumor tissue was calculated using the formula V=1/2×AB2 (mm^3) (a: long diameter; b: short diameter). The total volume of the tumor was equal to the sum of the single tumor volumes. The counting process was performed independently by two investigators (Xue and Han), and differences were resolved through consensus to obtain the final number.

H&E staining

The retained tissue samples were fixed in a 4% (w/v) paraformaldehyde solution for 24 h. Water was gradually removed from the tissue using. The paraffin in the sections was removed with xylene and then rehydrated with high and low concentrations of ethanol. The histological changes in tissues were observed under an optical microscope.

TUNEL cell apoptosis detection

Water was removed from the paraffin slices with xylene and ethanol. The samples were incubated with proteinase K at 37°C for 30 min, and 50 μl of TUNEL reaction solution was added to the tissue. Then, DAPI dye solution was added to the circle. Finally, the slices were observed under an inverted fluorescence microscope. The number of normal tumor cells and apoptotic tumor cells were counted using ImageJ software. The apoptosis index was calculated according to the following formula: apoptosis index = number of apoptotic tumor cells/(number of apoptotic tumor cells + number of normal tumor cells).

Statistical analysis

SPSS23.0 software was used for statistical analyses. All experimental data were expressed as the mean ± standard deviation (x±s). The overall data of multiple groups were compared using single-factor analysis of variance (ANOVA). The pairwise comparison between groups was analyzed by LSD-t-test. All *P* values were two-tailed, and *P* values <0.05 were considered statistically significant.

Results

Determination of hematoporphyrin concentrations

The average hematoporphyrin concentrations in normal and tumor pleural tissues were 3.965 and 7.854 μg/mg, respectively (**Figure 3**). The concentration of hematoporphyrin in tumor pleural tissues was significantly higher than that in normal pleura tissues, and the difference was statistically significant (P< 0.05).

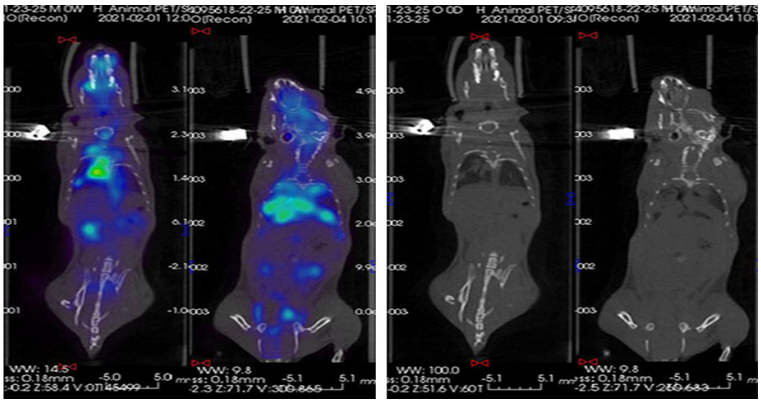

Figure 4. Comparison of PET-CT images before and after treatment in model control mice. By comparing the PET-CT images before and after treatment in the model control group, it can be seen that the volume of the tumor in the thoracic cavity was larger than before, and the area of the lung field was smaller than before.

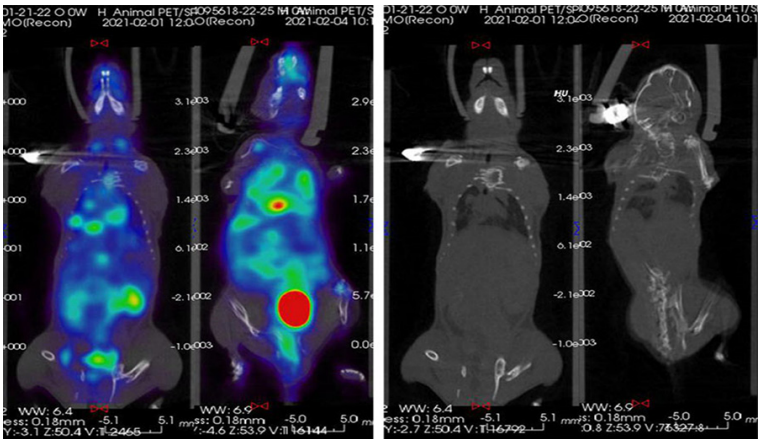

Figure 5. Comparison of PET-CT images before and after treatment in the PDT low-dose group. By comparing the PET-CT images before and after treatment in the PDT low-dose group, it can be seen that the volume of the tumor in the lung hilum reduced than before, and the area of the lung field increased than before.

In situ PDT could inhibit tumor growth

Eight days after the inoculation, the PET-CT images showed that there were multiple radioactive concentrated shadows in the thoracic cavity of mice, which were round or oval in size, and it could be concluded that the tumors were widely distributed on the right, tail, and ventral sides of the mice, and disseminated intrathoracic masses with a serosanguinous pleural effusion on both sides (**Figure 1**). For the mice with successfully established thoracic implant tumor models, the metastasis rate visible to the naked eye after dissection was 100%. By comparing the PET-CT images before and after treatment in each group, the tumor load of the PDT group was found to be significantly lower than those of the model control and pure laser irradiation groups. The PET-CT images of the model control group before and after treatment are shown in **Figure 4**. The PET-CT images of the low-dose PDT group before and after treatment are shown in **Figure 5**. The tumor volumes in the model control, pure laser irradiation, PDT low-dose, and PDT high-dose groups were 64.22±6.83, 61.75±13.26, 47.72±4.47, and 45.47±3.21 mm3, respectively. The differences in tumor volumes between the groups were statistically significant ($P<0.05$).

H&E staining results of normal pleural tissue

The H&E staining images of normal pleural tissues in each group are shown in **Figure 6**. Compared with the model control and pure laser irradiation groups, fractured fibrous tissue and a small amount of inflammatory cell infiltration were observed in the low-dose PDT group. Congested bleeding blood vessels and a large number of infiltrated inflammatory cells were observed in the high-dose PDT group.

The H&E staining results of tumor tissues

There were a large number of LLC cells in all four groups, which were closely arranged, with large H&E staining areas of tumor pleural tissue showing hyperchromatic nuclei and many nuclear fission images (**Figure 7**). The nuclei of the tumor cells were blue, the cytoplasms were red, and the interstitial staining was pink. Almost no necrotic tumor cells were observed in the model control group and the pure laser irradiation group. Punctate necrosis of tumor cells was observed in the low-dose PDT group. In the high-dose PDT group, the tumor cells were loosely arranged, the blood vessels were

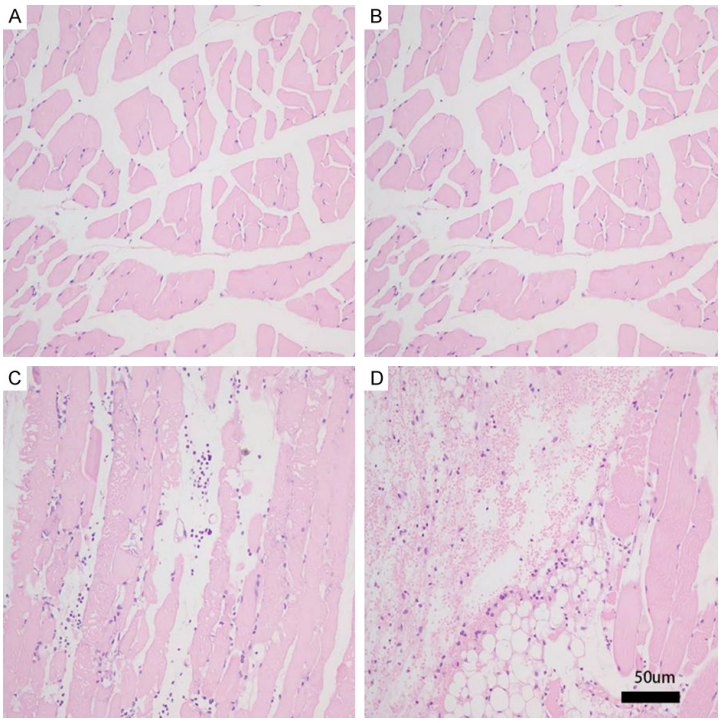

Figure 6. Histology of normal pleural tissues in each group under a microscope (×200). The nucleus was blue, and the cytoplasm was red. Compared with the model control group and pure laser irradiation group, the PDT low-dose group showed fractured fibrous tissue, a small amount of inflammatory cell infiltrated. The high-dose PDT group showed congested, bleeding blood vessels, and a large number of inflammatory cell infiltrated. A. Model control group. B. Pure laser irradiation group. C. PDT low dose group. D. PDT high dose group. Scalar bars: 50 um.

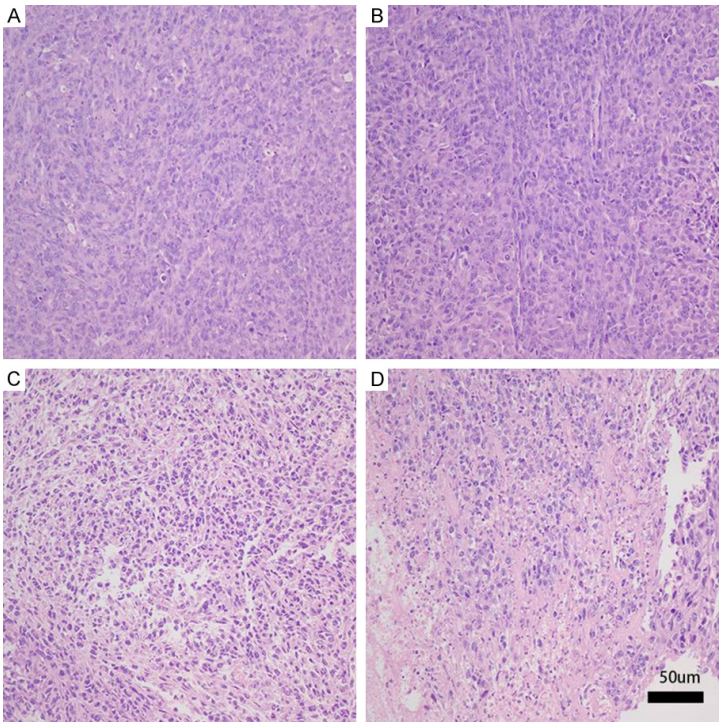

Figure 7. Histology of tumor tissues in each group under a microscope (×200). The nucleus was blue, the cytoplasm and interstitial staining was pink. There were a large number of tumors cells in the four groups, which were closely arranged, with large deeply stained nucleus and mitotic figures, suggesting that the thoracic implant tumor model was successfully established. There were almost no necrotic tumor cells in the model control group and pure laser irradiation group. There was punctate necrosis of tumor cells in the PDT low-dose group, and there was focal necrosis of tumor cells in the PDT high-dose group. A. Model control group. B. Pure laser irradiation group. C. PDT low dose group. D. PDT high dose group. Scalar bars: 50 um.

dilated and hyperemic, the nucleus was pyknotic, and focal necrosis of tumor cells was observed.

TUNEL apoptosis detection of tumor tissues

The TUNEL staining results of tumor tissues in each group are shown in **Figure 8**, where normal tumor nuclei are indicated by blue color, and apoptotic cells are indicated by green fluorescent staining. Apoptotic cells were scattered among the tumor cells. The apoptosis index of the model control group, pure laser irradiation group, PDT low-dose group, and PDT high-dose group were 6.33%±1.62, 9.25%±0.87, 26.68%±1.40, and 29.57%±2.73, respectively. The apoptosis index of the PDT group was significantly higher than those of the model control and pure laser irradiation groups, and the difference was statistically significant (**Figure 9**).

Discussion

To better represent the impact of the intrathoracic microenvironment on lung tumors, we performed intrathoracic inoculation of LLC cells to construct a thoracic implant tumor model. Based on the literature we have previously

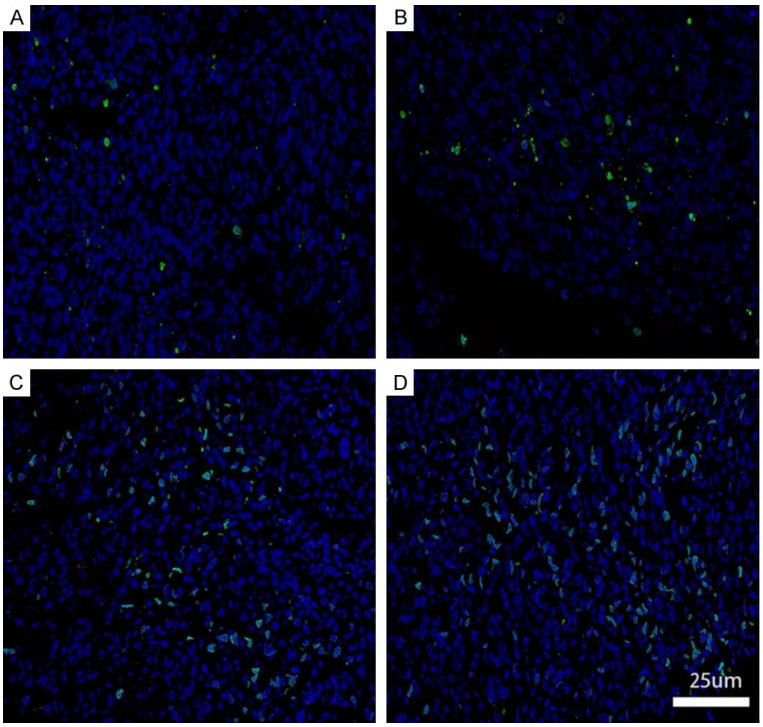

Figure 8. TUNEL apoptosis detection of tumor cells in each group (×400). Normal tumor cells were blue, and apoptotic cells were green fluorescent cells. Apoptotic cells were found in the tumor tissue in each group. The apoptotic cells were scattered among tumor cells. The number of apoptotic cells in the PDT group was significantly more than that of model control group and pure laser irradiation group. The number of apoptotic cells in the PDT high-dose group was more than that in the PDT low-dose group. A. Model control group. B. Pure laser irradiation group. C. PDT low-dose group. D. PDT high-dose group. Scalar bars: 25 um.

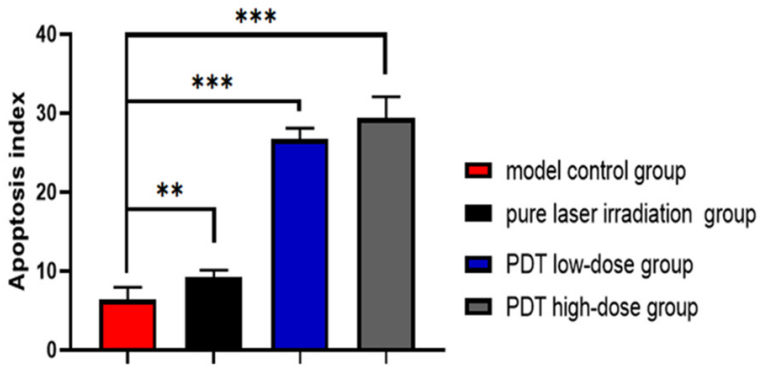

Figure 9. The apoptosis index of tumor cells in each group. The apoptosis index of the PDT group was significantly higher than those of the model control and pure laser irradiation groups, and the difference was statistically significant (***P<0.001, **P<0.01).

reviewed, it is easier to operate in the right thoracic cavity. Therefore, we decided to inoculate tumor cells and photosensitizers in the right thoracic cavity. Ten percent of the mice died when they were injected with tumor cells or photosensitizers. The death of mice usually occurred within the five minutes following the operation, which may be related to the puncture of large blood vessels or the heart or caused by pneumothorax or hemothorax.

When PDT is used to treat tumors clinically, intravenous administration is preferred. This method is easy to operate, but it produces systemic skin photosensitivity, and patients need to be protected from light for a long time after treatment. Thus, we locally administered the photosensitizer in the thoracic cavity to shorten the time between administration and laser irradiation. Our experimental results showed that hematoporphyrin accumulated specifically in the tumor tissue after topical administration.

Previous studies have shown that PDT can inhibit the growth of Lewis lung carcinoma tissue in mice [23]. By comparing the volume of tumors in groups, we concluded that PDT could inhibit tumor tissue growth and that the pure laser irradiation group had no obvious inhibitory effect on tumor tissue. There was punctate and focal necrosis of tumor cells in the PDT group, suggesting that PDT could cause tumor cell necrosis. TUNEL staining showed that PDT could induce apoptosis of tumor cells. As the concentration of the photosensitizer increased, the degree of apoptosis induced by PDT increased.

There are three main mechanisms of tumor cell death mediated by PDT *in vivo*: (1) The oxidative stress generated by PDT can directly cause tumor cell death; (2) PDT can damage the vascular system associated with the tumor, leading

to ischemia of the tumor tissue; and (3) PDT can activate acute inflammatory response and induce host defense immune response, thereby killing tumor cells [24]. Determination of the optimal conditions for PDT requires joint research in multiple disciplines such as physics, biology, chemistry, pharmacology, medicine, and other disciplines [25]. PDT can directly cause cell death through three pathways: apoptosis, necrosis, and autophagy. Apoptosis is a process in which chromatin condenses, DNA lyses into nucleosomes, cell atrophies, membrane blisters, and apoptotic bodies form. PDT can also induce non-apoptotic cell death by inducing autophagy [26].

In conclusion, this study explored the efficacy of intracavitary PDT on tumors *in situ* and its mechanism by establishing thoracic implant tumor models. The results showed that hematoporphyrin selectively accumulated in the pleural tumor tissue after local injection and that PDT via intrathoracic injection of photosensitizer can inhibit the growth of thoracic implant tumors in mice. Furthermore, the mechanism of tumor cell death may involve necrosis and apoptosis. The specific signal transduction pathways involved in the process require further investigation. A limitation of this study was that only a single light dose was adopted, so it was not possible to explore the effects of different light doses on tumor inhibition. Moreover, the duration of irradiation and the time interval between the administration of the photosensitizer and the irradiation, as well as the saturation point of the photosensitizer dose, may also affect the efficacy. PDT can also kill tumor cells by destroying the blood supply of tumors and generating immune responses. Due to the limited number of tumor specimens obtained in this experiment, further experiments are required to conduct in-depth investigations.

Acknowledgements

This work was supported by grants from the National Natural Scientific Foundation of China (No. 0030105).

Disclosure of conflict of interest

None.

Address correspondence to: Jing Feng and Nansheng Wan, Department of Respiratory and Critical Care Medicine, General Hospital of Tianjin Medical University, 154 Anshan Street, Tianjin 300052, China. E-mail: zyyhxkfj@126.com (JF); wnshzyy@163.com (NSW)

References

[1] Fenton KN and Richardson JD. Diagnosis and management of malignant pleural effusions. Am J Surg 1995; 170: 69-74.

[2] Fang LC, Komaki R, Allen P, Guerrero T, Mohan R and Cox JD. Comparison of outcomes for patients with medically inoperable stage I non-small-cell lung cancer treated with two-dimensional vs. three-dimensional radiotherapy. Int J Radiat Oncol Biol Phys 2006; 66: 108-116.

[3] Videtic GMM, Donington J, Giuliani M, Heinzerling J, Karas TZ, Kelsey CR, Lally BE, Latzka K, Lo SS, Moghanaki D, Movsas B, Rimner A, Roach M, Rodrigues G, Shirvani SM, Simone CB 2nd, Timmerman R and Daly ME. Stereotactic body radiation therapy for early-stage non-small cell lung cancer: executive summary of an ASTRO evidence-based guideline. Pract Radiat Oncol 2017; 7: 295-301.

[4] El-Sherif A, Gooding WE, Santos R, Pettiford B, Ferson PF, Fernando HC, Urda SJ, Luketich JD and Landreneau RJ. Outcomes of sublobar resectionversus lobectomy for stage I non-small cell lung cancer: a 13-year analysis. Ann Thorac Surg 2006; 82: 408-415.

[5] Bonnett R. Photodynamic therapy in historical perspective. Rev Contemp Pharmaco 1999; 1: 1-17.

[6] Dolmans DE, Fukumura D and Jain RK. Photodynamic therapy of cancer. Nat Rev Cancer 2003; 3: 380-387.

[7] Sakamaki Y, Ozdemir J, Heidrick Z, Azzun A, Watson O, Tsuji M, Salmon C, Sinha A, Batta-Mpouma J, McConnell Z, Fugitt D, Du YC, Kim JW and Beyzavi H. A bioconjugated chlorin-based metal-organic framework for targeted photodynamic therapy of triple negative breast and pancreatic cancers. ACS Appl Bio Mater 2021; 4: 1432-1440.

[8] Zou H, Wang FS, Zhou JJ, Liu X, He Q, Wang C, Zheng YW, Wen Y and Xiong L. Application of photodynamic therapy for liver malignancies. J Gastrointest Oncol 2020; 11: 431-442.

[9] Lu J, Yang L, Zhang W, Li P, Gao XN, Zhang W, Wang H and Tang B. The photodynamic therapy for hypoxic solid tumor via Mn-MOF as photosensitizer. Chem Commun (Camb) 2019; 55: 10792-10795.

[10] Chen B, Roskams T and de Witte PA. Antivascular tumor eradication by hypericin-mediated photodynamic therapy. Photochem Photobiol 2002; 76: 509-513.

[11] Wilson BC and Patterson MS. The physics, biophysics and technology of photodynamic therapy. Phys Med Biol 2008; 53: R61-109.

[12] Plaetzer K, Krammer B, Berlanda J, Berr F and Kiesslich T. Photophysics and photochemistry of photodynamic therapy: fundamental aspects. Lasers Med Sci 2009; 24: 259-268.
[13] Henderson BW and Dougherty TJ. How does Photodynamic therapy work? Photochem Photobiol 1992; 55: 145-157.
[14] Oleinick NL, Morris RL and Belichenko I. The role of apoptosis in response to photodynamic therapy: what, where, why, and how. Photochem Photobiol Sci 2002; 1: 1-21.
[15] Dąbrowski JM and Arnaut LG. Photodynamic therapy (PDT) of cancer: from local to systemic treatment. Photochem Photobiol Sci 2015; 14: 1765-1780.
[16] Kelly JF, Snell ME and Berenbaum MC. Photodynamic destruction of human bladder carcinoma. Br J Cancer 1975; 31: 237-244.
[17] Kao HW, Lin YY, Chen CC, Chi KH, Tien DC, Hsia CC, Lin WJ, Chen FD, Lin MH and Wang HE. Biological characterization of cetuximab-conjugated gold nanoparticles in a tumor animal model. Nanotechnology 2014; 25: 295102.
[18] Shafirstein G, Battoo A, Harris K, Baumann H, Gollnick SO, Lindenmann J and Nwogu CE. Photodynamic therapy of non-small cell lung cancer. Narrative review and future directions. Am Thorac Soc 2016; 13: 265-275.
[19] Calixto GM, Bernegossi J, de Freitas LM, Fontana CR and Chorilli M. Nanotechnology-based drug delivery systems for photodynamic therapy of cancer: a review. Molecules 2016; 21: 342.
[20] Sadanala KC, Chaturvedi PK, Seo YM, Kim JM, Jo YS, Lee YK and Ahn WS. Sono-photodynamic combination therapy: a review on sensitizers. Anticancer Res 2014; 34: 4657-4664.
[21] Manoto SL, Houreld NN and Abrahamse H. Resistance of lung cancer cells grown as multicellular tumour spheroids to zinc sulfophthalocyanine photosensitization. Int J Mol Sci 2015; 16: 10185-10200.
[22] Dolmans DE, Fukumura D and Jain RK. Photodynamic therapy for cancer. Nat Rev Cancer 2003; 3: 380-387.
[23] Chen B, Pogue BW, Zhou XD, O'Hara JA, Solban N, Demidenko E, Hoopes PJ and Hasan T. Effect of tumor host microenvironment on photodynamic therapy in a rat prostate tumor model. Clin Cancer Res 2005; 11: 720-727.
[24] Agostinis P, Berg K, Cengel KA, Foster TH, Girotti AW, Gollnick SO, Hahn SM, Hamblin MR, Juzeniene A, Kessel D, Korbelik M, Moan J, Mroz P, Nowis D, Piette J, Wilson BC and Golab J. Photodynamic therapy of cancer: an update. CA Cancer J Clin 2011; 61: 250-281.
[25] El-Hussein A, Manoto SL, Ombinda-Lemboumba S, Alrowaili ZA and Mthunzi-Kufa P. A review of chemotherapy and photodynamic therapy for lung cancer treatment. Anticancer Agents Med Chem 2021; 21: 149-161.
[26] Reiners JJ Jr, Agostinis P, Berg K, Oleinick NL and Kessel D. Assessing autophagy in the context of photodynamic therapy. Autophagy 2010; 6: 7-18.